

Quartz vein formation by local dehydration embrittlement along the deep, tremorgenic subduction thrust interface

Åke Fagereng^{1,2}, Johann F.A. Diener², Francesca Meneghini³, Chris Harris², and Ada Kvaldshem¹

¹School of Earth and Ocean Sciences, Cardiff University, Cardiff CF10 3AT, UK

²Department of Geological Sciences, University of Cape Town, Private Bag X3, Rondebosch 7701, South Africa

³Earth Science Department, University of Pisa, Pisa 56100, Italy

ABSTRACT

Hydrothermal quartz veins are ubiquitous in exhumed accretionary complexes, including the Namibian Damara belt. Here, subduction-related deformation occurred at temperatures ≤ 550 °C, and vein geometry is consistent with plate interface shear, low effective normal stresses, and mixed-mode deformation. Quartz vein $\delta^{18}\text{O}$ values relative to Standard Mean Ocean Water (SMOW) range from 9.4‰ to 17.9‰ ($n = 30$), consistent with precipitation from metamorphic fluids. A dominant subset of quartz veins away from long-lived high-strain zones and basaltic slivers have $\delta^{18}\text{O}$ values in a smaller range of 14.9‰ \pm 1‰, requiring precipitation from a fluid with $\delta^{18}\text{O}$ of 12‰ \pm 1‰ at 470–550 °C. This uniform fluid isotope value is consistent with progressive local breakdown of chlorite allowing extensive hydrofracture at temperatures typical of the plastic regime. In active subduction zones, brittle deformation within the plastic regime is inferred from observations of tectonic tremor, a noise-like seismic signal including overlapping low- and very low-frequency earthquakes, which occurs below the seismogenic zone. Both tremor and hydrothermal veins correlate with zones of inferred high fluid pressure, could represent a mixture of shear and dilatant failure, and may therefore be controlled by episodic hydrofracturing within a dominantly plastic and aseismic regime.

INTRODUCTION

Subducting sediments and oceanic crust experience increasing pressure (P) and temperature (T), triggering metamorphic dehydration reactions. It has been hypothesized that this dehydration creates extreme overpressures at the base of the subduction megathrust seismogenic zone (Saffer and Tobin, 2011). A consequence would be a localized zone of fluid-assisted deformation and, depending on stress conditions, formation of a hydrothermal vein system (e.g., Yardley, 1983). Here, we test whether an intense regionally developed vein system is consistent with fracture and vein growth in a relatively small P - T range related to prograde metamorphism. Our hypothesis test considers the geometry, microstructure, metamorphic conditions, and quartz oxygen isotope ratios of syntectonic veins throughout the nearly 80 km across-strike width of the exhumed accretionary complex of the Namibian Damara belt.

A fossil vein system formed at the base of the megathrust seismogenic zone should represent deformation recorded at similar conditions in active subduction zones, where geophysical observations indicate elevated fluid pressures (e.g., Shelly et al., 2006). Tectonic tremor has been reported within such inferred fluid overpressured zones in most well-instrumented subduction margins (Beroza and Ide, 2011). Tremor is defined as a weak, persistent, low-frequency (2–8 Hz) seismic signal that lasts for several days and repeats at regular intervals of several months (Obara, 2002).

The tremor signal includes low- and very low-frequency earthquakes with focal mechanisms indicating megathrust shear displacement (Ito et al., 2007; Shelly et al., 2007). However, shear displacement in low-frequency earthquakes cannot always explain the full tremor signal (Frank et al., 2014), which is also comparable to acoustic emissions observed during laboratory dehydration experiments (Burlini et al., 2009).

Both tectonic veins and tectonic tremor are hypothesized to result from fracture, healing by mineral precipitation, buildup of fluid pressure, and near-periodic repetition of this cycle (Yardley, 1983; Audet and Bürgmann, 2014). Quartz veins can form incrementally at length scales consistent with small stress drops in low-frequency earthquakes (Fagereng et al., 2011), and heal on time scales less than slow earthquake repeat times of weeks to months (Fisher and Brantley, 2014). Hayman and Lavier (2014) further calculated that local brittle failure within the plastic regime, as tremor represents, results in periodic slow slip events as commonly associated with tremor. We therefore hypothesize that syntectonic quartz veins within plastically deformed rocks may be a record of tremor, and discuss implications of this inference for fluid-mechanical processes at the tremor source.

GEOLOGICAL SETTING

The northeast-striking arm of the Damara belt formed during northwest-directed subduction

of the Khomas Sea underneath the Congo craton from ca. 580 Ma to 540 Ma (Miller, 1983; Meneghini et al., 2017). The high- T , low- P Central Zone (CZ) is interpreted as the volcanic arc, whereas the medium- T , medium- P Southern Zone (SZ) comprises metaturbidites and minor metabasites of mid-oceanic ridge basalt (MORB) affinity, interpreted as an accretionary prism (Figs. 1A–1C) (Gray et al., 2007; Meneghini et al., 2017). A foliation formed at

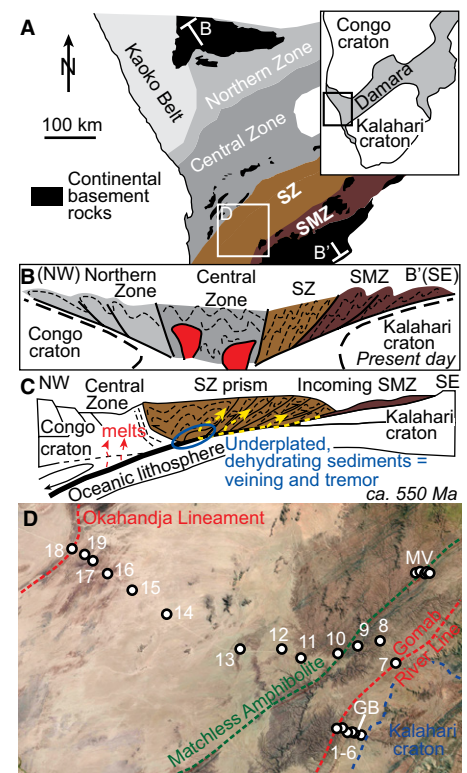


Figure 1. A: Simplified map of the inland branch of the Damara belt, Namibia, after Miller (1983). SZ—Southern Zone; SMZ—Southern Marginal Zone. B: Schematic cross section along line B-B' shown in A, modified from Gray et al. (2007). C: Reconstruction of margin during its subduction phase (modified after Meneghini et al., 2017), where dotted yellow arrows refer to particle paths in the prism (Moore et al., 2007). D: Sample locations and boundaries referred to in the text, depicted on Landsat satellite imagery. Numbers refer to sample numbers starting with KV in Table DR1 (see footnote 1).

$P \sim 1$ GPa and $540^\circ\text{C} < T < 560^\circ\text{C}$ is consistent with top-to-the-southeast kinematics and inferred to record peak subduction-related P - T conditions (Cross et al., 2015).

The Okahandja Lineament forms the northwest boundary between the SZ and the CZ, whereas the Gomab River Line separates the SZ from the Southern Marginal Zone (SMZ) in the southwest (Fig. 1D). The Matchless Amphibolite (MA) comprises tectonically imbricated metafacies rocks and metaturbidites, present at an approximately constant tectonostratigraphic level in the SZ for >350 km along strike (Miller, 1983). Meneghini et al. (2017) described the MA in detail and interpreted it as an imbricated ridge from the subducted Khomas Ocean. The SMZ is a zone of imbricate metasediments, metafacies slivers, and calc-silicate horizons, interpreted as the passive margin sequence on the Kalahari craton, accreted before the transition from oceanic subduction to continental collision (Miller, 1983).

We consider a transect from the southern edge of the SMZ through to the Okahandja Lineament (Fig. 1D): an 80 km horizontal distance through rocks dipping on average 45° northwest, equivalent to a true thickness of ~ 55 km neglecting any structural repetition. This represents the final thickness of an accretionary prism, which typically grows by successive underplating of subducted sediments and slices of oceanic crust that preserve structures formed along the megathrust (Kimura and Ludden, 1995; Moore et al., 2007) (Fig. 1C). In the SZ, Meneghini et al. (2017) recently demonstrated preservation of subduction-related structures that escaped overprint by exhumation, which in the Damara belt was largely accommodated on discrete structures such as the Okahandja Lineament.

HYDROTHERMAL VEINS

Ubiquitous hydrothermal quartz veins throughout the SZ and the SMZ are predominantly subparallel to the moderately northwest-dipping foliation (Fig. 2A). The veins are commonly folded by tight to isoclinal, asymmetric folds, with stretched, variably boudinaged limbs and locally isolated hinges (Fig. 2B). Hinge surfaces are roughly foliation-parallel, and veins both crosscut and deflect the foliation (Figs. 2A and 2B). In places, foliation-parallel veins and foliation-oblique veins are mutually crosscutting and accommodate both shear and dilation (Fig. 2C). Quartz veins also occur in boudin necks of plastically deformed, competent lenses of metachert, quartzite, or metabasite, and in places the veined boudin neck is itself boudinaged (Fig. 2D).

The veins are blocky at the mesoscale, and at the microscale comprise quartz crystals of millimeters to centimeters in diameter (Fig. 2E). Grain boundaries are sutured, and local subgrains occur along grain boundaries (Figs. 2E and 2F). The dominance of grain boundary

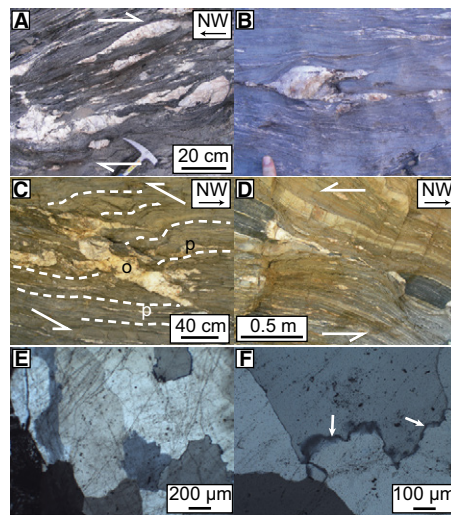


Figure 2. Photographs of quartz veins in Kuiseb Schist (Damara belt, Namibia). White arrows in panels A, C, and D show inferred sense of shear. A: Typical outcrop appearance of folded and boudinaged, foliation-parallel veins. B: Isoclinal fold in vein parallel to, and crosscut by, greenschist facies foliation. C: Mutually crosscutting foliation-parallel (p) and foliation-oblique (o) veins; foliation traces in white dashed lines. D: Boudinaged metamafic lens and quartz vein. E: Photomicrograph showing serrated vein quartz grain boundaries and inclusion trails across these boundaries (sample KV18). F: Photomicrograph of vein quartz grain boundary with recrystallized grains (white arrows) (sample GBLC). Both photomicrographs were taken in cross-polarized light.

migration microstructures, with rare evidence for subgrain and bulging recrystallization, is typical of natural quartz deformation at $T > 500^\circ\text{C}$ (Stipp et al., 2002). Solid and fluid inclusion bands are common, with variable spacing and orientation, although a dominant orientation can be determined locally (Figs. 2E and 2F).

Following Fagereng et al. (2014), we interpret the ubiquitous foliation-parallel and plastically

deformed veins, and foliation-oblique veins in mutually crosscutting relationship with the foliation-parallel veins (Fig. 2C), to have formed at the same time as the tectonic, subduction-related foliation. Accepting the hypothesis that accretionary prisms form by successive underplating of packages hundreds of meters in thickness (Kimura and Ludden, 1995), these veins represent top-to-the-southeast, dilatant shear within or close to the subduction thrust interface (Figs. 1C, 2A, and 2C). Locally, e.g., along the Okahandja Lineament, veined rock assemblages are deformed by later faults related to exhumation within the prism.

METHODS

Analyses of quartz veins were performed at the University of Cape Town (South Africa) using the laser fluorination method of Harris and Vogeli (2010), where 2–3 mg clean quartz chips were reacted with BrF_5 and collected as O_2 . Raw data were converted to δ -notation relative to standard mean ocean water (SMOW) based on an internal garnet standard (MON GT; $\delta^{18}\text{O} = 5.38\text{‰}$). The long-term difference in $\delta^{18}\text{O}$ values of two MON GT standards run with each batch of 10 samples is 0.12‰ ($n = 216$), corresponding to a 2σ value of 0.15‰ .

Assuming burial along a profile shaped as predicted by the analytical thermal model of Molnar and England (1990), and intersecting metamorphic P - T conditions reported for the Damara accretionary prism (Cross et al., 2015), we assess the fluid release from an underthrust package during subduction (Fig. 3). Fluid production is calculated for a metapelite, the volumetrically dominant lithology within the SZ and SMZ (Fig. 3A), and the mafic component of the MA (Fig. 3B). We use THERMOCALC version 3.45 (<http://www.metamorph.geo.uni-mainz.de/thermocalc/>), with the thermodynamic data set of Holland and Powell (2011; data set 6.2, created 6 February 2012) and activity-composition

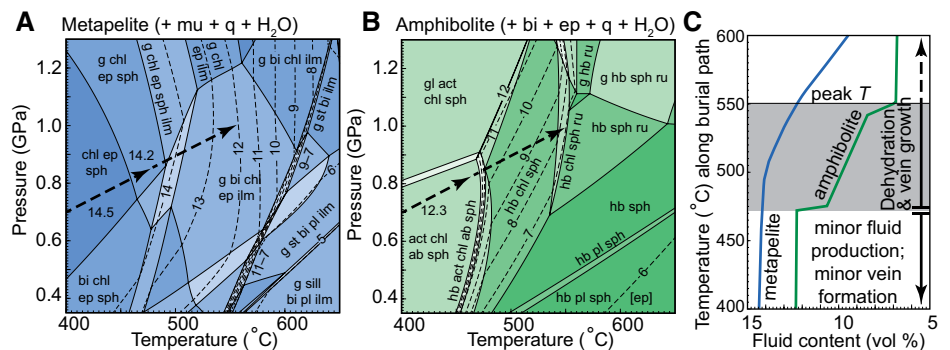


Figure 3. A, B: Pseudosections for metapelite (A) and amphibolite (B) compositions, contoured for volume percent fluid held in mineral assemblage (thin dashed lines). C: Fluid production along subduction burial path, shown as thick dashed arrow in A and B, with very limited fluid release below temperatures of 470°C , followed by punctuated and steady fluid release to peak temperatures (T). Mineral abbreviations: ab—albite; act—actinolite; bi—biotite; chl—chlorite; ep—epidote; g—garnet; gl—glaucophane; hb—hornblende; ilm—ilmenite; mu—muscovite; pl—plagioclase; q—quartz; ru—rutile; sill—sillimanite; sph—titanite; st—staurolite.

relations of White et al. (2014) and Green et al. (2016).

METAMORPHIC FLUID RELEASE

Along the estimated P - T path, very little fluid is released at $T < 470$ °C, as all low-grade hydrous minerals remain stable (Figs. 3A–3C). At 470 °C, biotite is introduced in the metapelite, and hornblende becomes stable in the amphibolite (Figs. 3A and 3B). In both cases, new mineral growth consumes chlorite. Fluid production in the metapelite is continuous but gradual as chlorite is consumed with increasing T to the reported peak conditions of 550 °C, with ~2.2 vol% fluid released over this section of the P - T path (Fig. 3C). The amphibolite initially experiences voluminous dehydration and fluid release, with ~2 vol% fluid produced at 470–475 °C as actinolite and albite are exhausted (Fig. 3B), before continued consumption of chlorite yields a further 3 vol% fluid as 550 °C is approached.

If the rocks are sufficiently impermeable to prevent flow along, into, or out of the fault zone, the calculations predict few veins to form below 470 °C, whereas numerous veins form as the rocks are heated from 470 to 550 °C (Fig. 3C). This is consistent with the observation of plastically deformed veins crosscutting a foliation defined by minerals stable at $T > 470$ °C (Fig. 2)

VEIN AND FLUID OXYGEN ISOTOPE COMPOSITIONS

Vein quartz $\delta^{18}\text{O}$ values vary from 9.4‰ to 17.9‰ ($n = 30$) (Fig. 4A; Table DR1 in the GSA

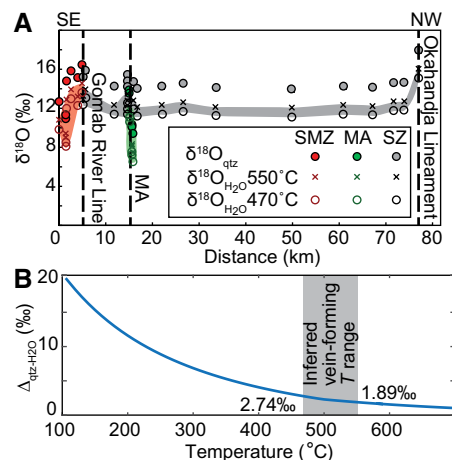


Figure 4. A: Quartz vein $\delta^{18}\text{O}$ values as function of across-strike distance from the structural base of the Southern Marginal Zone, Damara belt, Namibia (Fig. 1). Calculated fluid $\delta^{18}\text{O}$ values, also plotted against distance, are based on fluid release temperatures of 470–550 °C. **B:** Quartz-water fractionation factor, after Matsuhisa et al. (1979) as a function of temperature, with values used for calculations in A indicated by gray shading. SMZ—Southern Marginal Zone; MA—Matchless amphibolite; SZ—Southern Zone; qtz—quartz.

Data Repository¹). Throughout the SZ, quartz vein $\delta^{18}\text{O}$ values are within a 2.0‰ range from 13.9‰ to 15.9‰ ($n = 13$). The MA veins show lower quartz $\delta^{18}\text{O}$ values, ranging from 9.4‰ to 15.4‰ ($n = 8$); also, the SMZ has a larger range in quartz vein $\delta^{18}\text{O}$ values, from 10.9‰ to 16.4‰ ($n = 8$). A sample from the Okahandja Lineament has $\delta^{18}\text{O}$ of 17.9‰, the highest value in this study. The difference between samples of mutually crosscutting veins oblique and subparallel to schistose foliation is <1.0 ‰ (Table DR1).

Vein $\delta^{18}\text{O}$ is controlled by precipitation T and the $\delta^{18}\text{O}$ of the fluid from which quartz precipitated. The difference between quartz and water $\delta^{18}\text{O}$ values ($\Delta_{\text{qtz-H}_2\text{O}}$) approximates $a \times (10^6 T^{-2}) - b$, where a and b are empirical constants (determined by Matsuhisa et al., 1979). From the metamorphic constraints (Fig. 3), we explore the T window from 470 °C to 550 °C, where the T -dependent $\Delta_{\text{qtz-H}_2\text{O}}$ values are 2.7‰ to 1.9‰, respectively (Fig. 4B). Within the SZ, the inferred fluid $\delta^{18}\text{O}$ is 11‰–13‰, whereas measured quartz $\delta^{18}\text{O}$ in the SMZ and MA require fluid $\delta^{18}\text{O}$ as low as 8‰ and 6.5‰ respectively, if precipitation occurred at 470 °C (Fig. 4A). The elevated quartz $\delta^{18}\text{O}$ in the Okahandja Lineament requires a fluid $\delta^{18}\text{O}$ of 15‰–16‰ or precipitation at lower T .

VEIN-FORMING CONDITIONS

The value of $\Delta_{\text{qtz-H}_2\text{O}}$ decreases with increasing T (Fig. 4B); therefore, if seawater ($\delta^{18}\text{O} = 0$ ‰ \pm 2‰) is trapped in subducting sediments and released gradually with depth, quartz precipitated from this pore fluid tracks a gradient from high to low values with increasing T of precipitation. O’Hara et al. (1997) found quartz $\delta^{18}\text{O}$ values decreasing from 17.8‰ to 3.4‰ with increasing metamorphic grade along a transect through the Altyn Tagh accretionary complex, China, and interpreted these veins as formed progressively from pore fluid release. In the SZ, such a gradient is not observed. Instead, calculated fluid $\delta^{18}\text{O}$ has a narrow range of 12‰ \pm 1‰ (Fig. 4), similar to 13‰ \pm 1‰ calculated for fluids from which quartz precipitated across blueschist- to amphibolite-facies units in the Catalina Schist (Santa Catalina Island, California; Bebout, 1991). These values are consistent with precipitation from fluids in equilibrium with trench and ocean-floor metasediments (10‰–20‰; Savin and Epstein, 1970), at a T where $\Delta_{\text{qtz-H}_2\text{O}}$ is small.

Quartz vein $\delta^{18}\text{O}$ values from the MA are lower than in the metasedimentary SZ. Basalts have lower bulk-rock $\delta^{18}\text{O}$ than shale (< 8 ‰; Muehlenbachs, 1986); relatively low quartz-vein $\delta^{18}\text{O}$ is therefore expected where fluid $\delta^{18}\text{O}$ is buffered by host metabasites. In the SMZ, $\delta^{18}\text{O}$

values are also lower than in the SZ. This can partially be explained by local presence of metabasalt; in addition, the range of passive margin sediments would also have provided a range of fluid compositions. Higher quartz vein $\delta^{18}\text{O}$ values in the Okahandja Lineament can be explained by larger $\Delta_{\text{qtz-H}_2\text{O}}$ as deformation and fluid flow persisted to lower temperatures in this high-strain zone.

In summary, the majority of quartz vein $\delta^{18}\text{O}$ values are consistent with precipitation at 470–550 °C from locally released metamorphic fluids (Fig. 3). To be consistent in composition across the prism, this fluid release likely occurred within subducting sediments along the plate interface, before incorporation into the prism by underplating and downward migration of the megathrust (Fig. 1C).

DEHYDRATION, DEFORMATION, AND TECTONIC TREMOR

At the vein-forming conditions, metamorphic fluids were released into low-permeability rocks where fluid overpressure gradually developed until hydrofracture could occur (Yardley, 1983). That the dominant vein orientation is parallel to foliation (Figs. 2A–2D) implies the tensile strength along foliation was exceeded before the tensile strength of intact rock. Exceptions to this are foliation-oblique veins associated with mixed-mode dilational shear failure, e.g., where foliation is deflected with a reverse sense of shear along a dilatant fracture (Fig. 2C). Thus, the vein system accommodated both tensile failure, requiring fluid pressure in excess of the least compressive stress, and dilational shear, which could have produced space and pressure drops for quartz precipitation without requiring hydrofracture conditions (Lewis and Byrne, 2003). Foliation-parallel shear failure may also well have occurred, but would be near impossible to recognize given lack of marker horizons (Fagereng et al., 2014).

In active subduction zones, tectonic tremor events repeat within a particular depth range (e.g., Beroza and Ide, 2011), which may relate to metamorphic dehydration reactions whose depth depends on the local geothermal gradient (Fagereng and Diener, 2011). Local dehydration at $\gg 350$ °C creates intensive brittle deformation in the plastic regime at a location dependent on local thermal structure, not necessarily coincident with the frictional-plastic transition zone (Gao and Wang, 2017), but critically dependent on where dehydration and silicification occur (Audet and Bürgmann, 2014; Hyndman et al., 2015). We suggest that the Damara quartz veins record silicification of subducting sediments, which may also have promoted their underplating and preservation by hardening of the underthrust plastically weak, fine-grained assemblage. If the vein-forming process is analogous to tremor, the noisy part of the tremor

¹GSA Data Repository item 2018015, Table DR1 (sample locations and oxygen isotope values), is available online at <http://www.geosociety.org/datarepository/2018/> or on request from editing@geosociety.org.

signal may represent tensile hydrofracture and vein formation in intact rock, whereas low- and very low-frequency earthquakes are associated with low-effective-stress shear failure as occurs along fluid-overpressured, vein-coated, weak foliation planes (Fagereng et al., 2011). In this interpretation of the tremor source, the regular repeat time of episodic tremor and slow slip events may arise from a regular cycle of fluid pressure-driven failure—where a combination of fracture healing and fluid production rates determines repeat times (Audet and Bürgmann, 2014; Fisher and Brantley, 2014).

ACKNOWLEDGMENTS

Fieldwork and isotope analyses were supported by University of Cape Town Research Development grants to Fagereng and Diener, and a Claude Leon Foundation grant to Meneghini at Stellenbosch University (South Africa). Fagereng is supported by European Research Council starting grant 715836 “MICA”. We thank J.C. Lewis and N. Hayman for critical comments that significantly improved the manuscript.

REFERENCES CITED

Audet, P., and Bürgmann, R., 2014, Possible control of subduction zone slow-earthquake periodicity by silica enrichment: *Nature*, v. 510, p. 389–392, <https://doi.org/10.1038/nature13391>.

Bebout, G.E., 1991, Field-based evidence for devolatilization in subduction zones: Implications for arc magmatism: *Science*, v. 251, p. 413–416, <https://doi.org/10.1126/science.251.4992.413>.

Beroza, G.C., and Ide, S., 2011, Slow earthquakes and nonvolcanic tremor: *Annual Review of Earth and Planetary Sciences*, v. 39, p. 271–296, <https://doi.org/10.1146/annurev-earth-040809-152531>.

Burlini, L., Di Toro, G., and Meredith, P., 2009, Seismic tremor in subduction zones: Rock physics evidence: *Geophysical Research Letters*, v. 36, L08305, <https://doi.org/10.1029/2009GL037735>.

Cross, C.B., Diener, J.F.A., and Fagereng, Å., 2015, Metamorphic imprint of accretion and ridge subduction in the Pan-African Damara Belt, Namibia: *Journal of Metamorphic Geology*, v. 33, p. 633–648, <https://doi.org/10.1111/jmg.12139>.

Fagereng, Å., and Diener, J.F.A., 2011, Non-volcanic tremor and discontinuous slab dehydration: *Geophysical Research Letters*, v. 38, L15302, <https://doi.org/10.1029/2011GL048214>.

Fagereng, Å., Remitti, F., and Sibson, R.H., 2011, Incrementally developed slickenfibers—Geological record of repeating low stress-drop seismic events?: *Tectonophysics*, v. 510, p. 381–386, <https://doi.org/10.1016/j.tecto.2011.08.015>.

Fagereng, Å., Hillary, G.W., and Diener, J.F., 2014, Brittle-viscous deformation, slow slip, and tremor: *Geophysical Research Letters*, v. 41, p. 4159–4167, <https://doi.org/10.1002/2014GL060433>.

Fisher, D.M., and Brantley, S.L., 2014, The role of silica redistribution in the evolution of slip instabilities along subduction interfaces: Constraints from the Kodiak accretionary complex, Alaska: *Journal of Structural Geology*, v. 69, p. 395–414, <https://doi.org/10.1016/j.jsg.2014.03.010>.

Frank, W.B., Shapiro, N.M., Husker, A.L., Kostoglodov, V., Romanenko, A., and Campillo, M., 2014, Using systematically characterized low-frequency earthquakes as a fault probe in

Guerrero, Mexico: *Journal of Geophysical Research: Solid Earth*, v. 119, p. 7686–7700, <https://doi.org/10.1002/2014JB011457>.

Gao, X., and Wang, K., 2017, Rheological separation of the megathrust seismogenic zone and episodic tremor and slip: *Nature*, v. 543, p. 416–419, <https://doi.org/10.1038/nature21389>.

Gray, D.R., Foster, D.A., Maas, R., Spaggiari, C.V., Gregory, R.T., Goscombe, B., and Hoffman, K.H., 2007, Continental growth and recycling by accretion of deformed turbidite fans and remnant ocean basins: Examples from Neoproterozoic and Phanerozoic orogens, in Hatcher, R.D., Jr., et al., eds., 4-D Framework of Continental Crust: Geological Society of America Memoir 200, p. 63–92, [https://doi.org/10.1130/2007.1200\(05\)](https://doi.org/10.1130/2007.1200(05)).

Green, E.C.R., White, R.W., Diener, J.F.A., Powell, R., Holland, T.J.B., and Palin, R.M., 2016, Activity–composition relations for the calculation of partial melting equilibria in metabasic rocks: *Journal of Metamorphic Geology*, v. 34, p. 845–869, <https://doi.org/10.1111/jmg.12211>.

Harris, C., and Vogeli, J., 2010, Oxygen isotope composition of garnet in the Peninsula Granite, Cape Granite Suite, South Africa: Constraints on melting and emplacement mechanisms: *South African Journal of Geology*, v. 113, p. 401–412, <https://doi.org/10.2113/gssajg.113.4.401>.

Hayman, N., and Lavier, L.L., 2014, The geological record of deep episodic tremor and slip: *Geology*, v. 42, p. 195–198, <https://doi.org/10.1130/G34990.1>.

Holland, T.J.B., and Powell, R., 2011, An improved and extended internally consistent thermodynamic dataset for phases of petrological interest, involving a new equation of state for solids: *Journal of Metamorphic Geology*, v. 29, p. 333–383, <https://doi.org/10.1111/j.1525-1314.2010.00923.x>.

Hyndman, R.D., McCrory, P.A., Wech, A., Kao, H., and Ague, J., 2015, Cascadia subducting plate fluids channelled to fore-arc mantle corner: ETS and silica deposition: *Journal of Geophysical Research: Solid Earth*, v. 120, p. 4344–4358, <https://doi.org/10.1002/2015JB011920>.

Ito, Y., Obara, K., Shiomi, K., Sekine, S., and Hirose, H., 2007, Slow earthquakes coincident with episodic tremors and slow slip events: *Science*, v. 315, p. 503–506, <https://doi.org/10.1126/science.1134454>.

Kimura, G., and Ludden, J., 1995, Peeling oceanic crust in subduction zones: *Geology*, v. 23, p. 217–220, [https://doi.org/10.1130/0091-7613\(1995\)023<0217:POCISZ>2.3.CO;2](https://doi.org/10.1130/0091-7613(1995)023<0217:POCISZ>2.3.CO;2).

Lewis, J.C., and Byrne, T.B., 2003, History of metamorphic fluids along outcrop-scale faults in a Paleogene accretionary prism, SW Japan: Implications for prism-scale hydrology: *Geochemistry Geophysics Geosystems*, v. 4, 9007, <https://doi.org/10.1029/2002GC000359>.

Matsuhisa, Y., Goldsmith, J.R., and Clayton, R.N., 1979, Oxygen isotopic fractionation in the system quartz-albite-anorthite-water: *Geochimica et Cosmochimica Acta*, v. 43, p. 1131–1140, [https://doi.org/10.1016/0016-7037\(79\)90099-1](https://doi.org/10.1016/0016-7037(79)90099-1).

Meneghini, F., Fagereng, Å., and Kisters, A., 2017, The Matchless Amphibolite of the Damara belt, Namibia: Unique preservation of a late Neoproterozoic ophiolitic suture: *Ophioliti*, v. 42, p. 129–145, <https://doi.org/10.4454/ofioliti.v42i2.488>.

Miller, R.McG., 1983, Evolution of the Damara Orogen of Southwest Africa/Namibia: Geological Society of South Africa Special Publication 11, 515 p.

Molnar, P., and England, P., 1990, Temperatures, heat flux, and frictional stress near major thrust faults: *Journal of Geophysical Research*, v. 95, p. 4833–4856, <https://doi.org/10.1029/JB095iB04p04833>.

Moore, J.C., Rowe, C., and Meneghini, F., 2007, How accretionary prisms elucidate seismogenesis in subduction zones, in Dixon, T.H., and Moore, J.C., eds., *The Seismogenic Zone of Subduction Thrust Faults*: New York, Columbia University Press, p. 288–315, <https://doi.org/10.7312/dixo13866-010>.

Muehlenbachs, K., 1986, Alteration of oceanic crust and the ^{18}O history of seawater, in Valley, J.W., et al., eds., *Stable Isotopes in High Temperature Geological Processes*: Washington, D.C., Mineralogical Society of America, *Reviews in Mineralogy*, v. 16, p. 425–444.

Obara, K., 2002, Nonvolcanic deep tremor associated with subduction in southwest Japan: *Science*, v. 296, p. 1679–1681, <https://doi.org/10.1126/science.1070378>.

O’Hara, K.D., Yang, X.Y., Guoyuan, X., and Li, Z., 1997, Regional $\delta^{18}\text{O}$ gradients and fluid-rock interaction in the Altay accretionary complex, northwest China: *Geology*, v. 25, p. 443–446, [https://doi.org/10.1130/0091-7613\(1997\)025<0443:ROGAFR>2.3.CO;2](https://doi.org/10.1130/0091-7613(1997)025<0443:ROGAFR>2.3.CO;2).

Saffer, D.M., and Tobin, H.J., 2011, Hydrogeology and mechanics of subduction zone forearcs: Fluid flow and pore pressure: *Annual Review of Earth and Planetary Sciences*, v. 39, p. 157–186, <https://doi.org/10.1146/annurev-earth-040610-133408>.

Savin, S.M., and Epstein, S., 1970, The oxygen and hydrogen isotope geochemistry of ocean sediments and shales: *Geochimica et Cosmochimica Acta*, v. 34, p. 43–63, [https://doi.org/10.1016/0016-7037\(70\)90150-X](https://doi.org/10.1016/0016-7037(70)90150-X).

Shelly, D.R., Beroza, G.C., Ide, S., and Nakamura, S., 2006, Low-frequency earthquakes in Shikoku, Japan, and their relationship to episodic tremor and slip: *Nature*, v. 442, p. 188–191, <https://doi.org/10.1038/nature04931>.

Shelly, D.R., Beroza, G.C., and Ide, S., 2007, Non-volcanic tremor and low-frequency earthquake swarms: *Nature*, v. 446, p. 305–307, <https://doi.org/10.1038/nature05666>.

Stipp, M., Stünitz, H., Heilbronner, R., and Schmid, S.M., 2002, Dynamic recrystallization of quartz: Correlation between natural and experimental conditions, in De Meer, S., et al., eds., *Deformation Mechanisms, Rheology and Tectonics: Current Status and Future Perspectives*: Geological Society of London Special Publication 200, p. 171–190, <https://doi.org/10.1144/GSL.SP.2001.200.01.11>.

White, R.W., Powell, R., and Johnson, T.E., 2014, The effect of Mn on mineral stability in metapelites revisited: New $a-x$ relations for manganese-bearing minerals: *Journal of Metamorphic Geology*, v. 32, p. 809–828, <https://doi.org/10.1111/jmg.12095>.

Yardley, B., 1983, Quartz veins and devolatilization during metamorphism: *Journal of the Geological Society*, v. 140, p. 657–663, <https://doi.org/10.1144/gsjgs.140.4.0657>.

Manuscript received 23 August 2017

Revised manuscript received 19 October 2017

Manuscript accepted 23 October 2017

Printed in USA